Building a robust 3D Ca-MOF by a new square Ca_4O SBU for purification of natural gas

Falu Hu,[ab] Zhengyi Di,[c] Mingyan Wu,[c*] and Jing Li [ba*]

[a] Hoffmann Institute of Advanced Materials, Shenzhen Polytechnic, 7098 Liuxian Blvd, Nanshan District, Shenzhen, 518055, China.
[b] Department of Chemistry and Chemical Biology, Rutgers University, 123 Bevier Road, Piscataway, NJ, 08854, USA
[c] State Key Laboratory of Structure Chemistry, Fujian Institute of Research on the Structure of Matter, Chinese Academy of Sciences, Fuzhou, 350002, China
E-mail: wumy@fjirsm.ac.cn.
E-mail: jingli@rutgers.edu

Experimental Section

Materials and methods

All reagents and solvents used in synthesis are commercially available and used as supplied without further purification. Single crystal X-ray diffraction experiments were performed on a Bruker D8-Venture diffractometer equipped with a Cu microfocus tube (λ = 1.54178 Å). Powder X-ray diffraction (PXRD) analyses were carried out on a Rigaku Ultima-IV unit using Cu Ka radiation (λ = 1.54178 Å). Thermogravimetric analyses were recorded on a Q5000IR unit at a heating rate of 10 ºC min^{-1} under nitrogen atmosphere. Gas sorption isotherms of activated **1** were measured on a 3FLEX unit. The breakthrough experiments for mixed gas CO_2 / CH_4, C_2H_6 / CH_4 and C_3H_8 / CH_4 (15±0.5:85±0.5) were carried out at a flow rate of 2 ml / min (298 K, 1 bar) using a home-built setup coupled with a GC-9860-5CNJ. Activated sample **1** in powder form (65 mm and 391 mg) was packed into stainless-steel column ϕ 3 X 180 mm in glove box. Before the breakthrough experiments, the correction factors of CO_2/CH_4, C_2H_6/CH_4 and C_3H_8/CH_4 (15±0.5:85±0.5) were obtained. The binary mixture gas with a flow rate of 2 ml / min (298 K, 1 bar) was then introduced through the bypass line with a resistance. The sample was activated at 80 ºC with 20 ml / min He flow for 10 h followed by flowing CO_2/CH_4, C_2H_6/CH_4 and C_3H_8/CH_4 binary gas mixtures through the alternative vent line for 30 min before introducing into the adsorption column.

Calculation of isosteric heats of adsorption

We test the adsorption isotherms of various gases from low pressure to 1 bar at 298 K and 273 K, respectively. And then we used the equation (1) to fit the 298 K and 273 K data. Finally, we used the equation (2) to calculate the isosteric heats of adsorption according to the fitting parameters.

$$\ln P = \ln N + \left(\frac{1}{T}\right)\sum_{i=0}^{m} a_i \times N^i + \sum_{j=0}^{n} b_j \times N^j \quad (1)$$

P : pressure (mmHg),
N : the amount adsorbed (mg/g),
T : temperature (K),
a_i and b_j: parameters
R: the universal gas constant (8.314 J • mol^{-1} • K^{-1})
m and n determine the number of terms required to adequately describe the isotherm the isosteric heat of adsorption is calculated according to:

$$Q_{st} = -R\sum_{i=0}^{m} a_i \times N^i \quad (2)$$

Synthesis of $[Me_2NH_2^+]_2[Ca_4O(MTB)_2(CH_3CH_2OH)_4]\cdot(solvent)_n$ (1)

$Ca(NO_3)_2\cdot 4H_2O$ (0.1mmol) and H_4MTB (0.01mmol) in the mixture solvents of DMF (2ml) and EtOH (0.5ml) were charged in a Pyrex vial at 80 ºC for 5 days. Colorless crystals were collected after the reaction (Yield: 50% based on the ligand).

Sample activation procedure

The bulk sample (about 100 mg) was pretreated by soaking the crystals of **1** in super-dry EtOH for 3 days at room temperature. The solution was refreshed three times daily during this time period. The sample was then degassed under dynamic high vacuum (6.7 Pa) at 80 ºC for 10 h to afford the activated desolvated sample. The activated sample was transferred to a tube and degassed under dynamic high vacuum (5 mmHg) at 80 ºC for 10 h. Single-component gas sorption isotherms were then carried out on the sample at 273K and 298K, respectively.

Figures

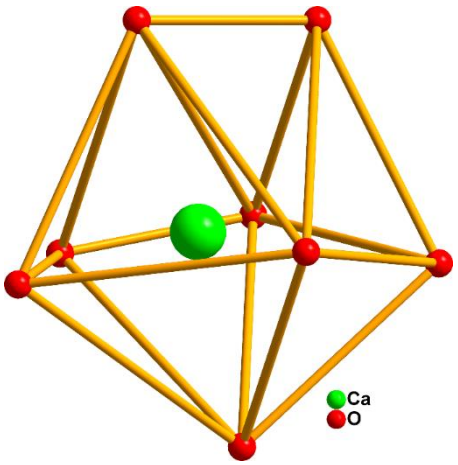

Fig. S1. The trigonal dodecahedron geometry of Ca^{2+}.

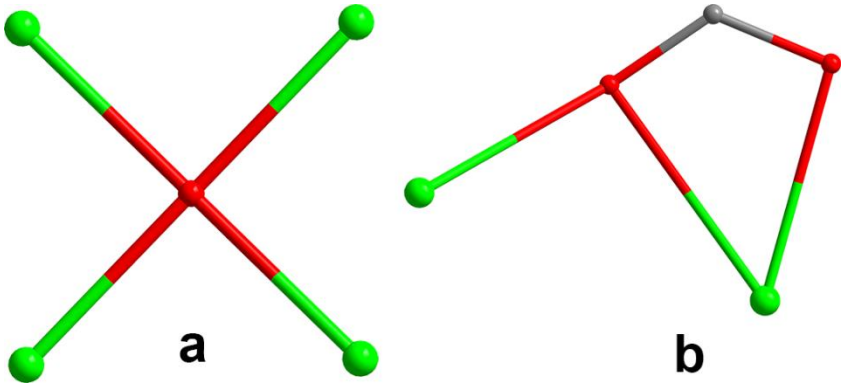

Fig. S2. Two coordination modes of oxygen atoms in **1**.

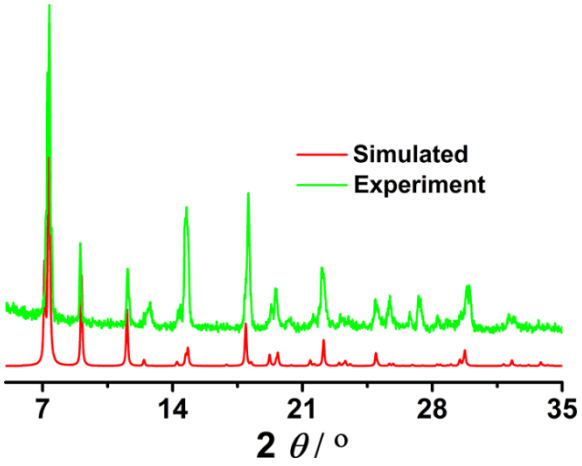

Fig. S3. Experimental and simulated PXRD patterns of **1**.

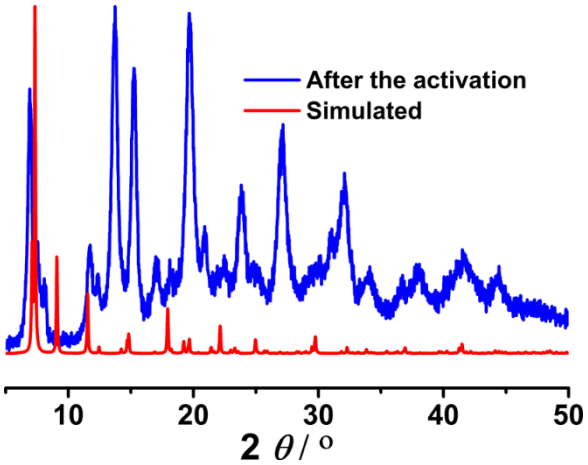

Fig. S4. Experimental PXRD patters of activated sample **1** in comparison with the simulated pattern.

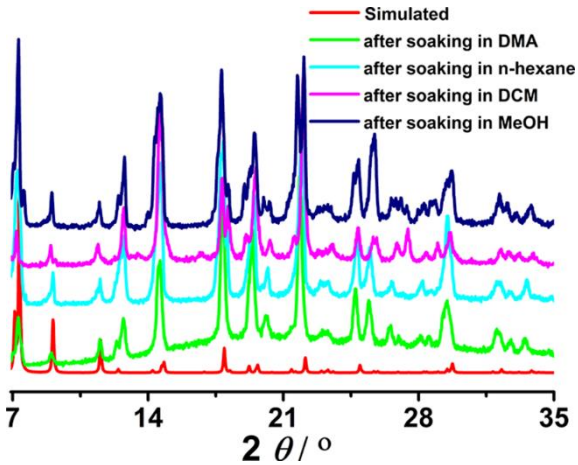

Fig. S5. PXRD patterns of **1** after being soaked in various solvents for 24h. The simulated PXRD pattern (red) is included for comparison.

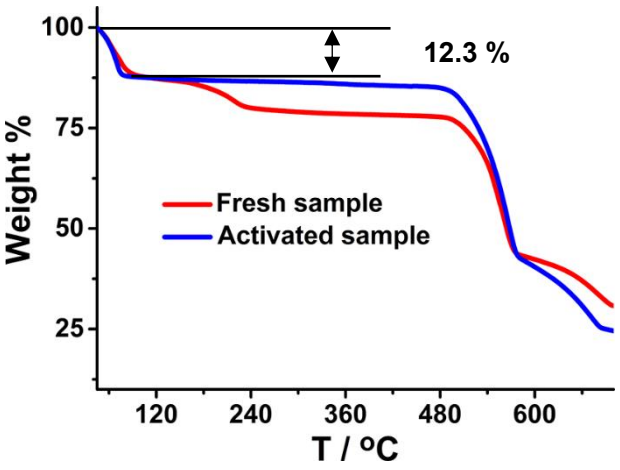

Fig. S6. The TGA curves of the fresh and activated sample, respectively.

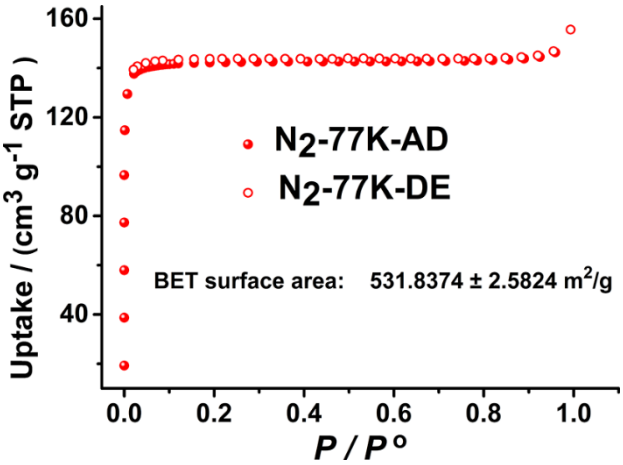

Fig. S7. The N_2 adsorption-desorption isotherms of **1**.

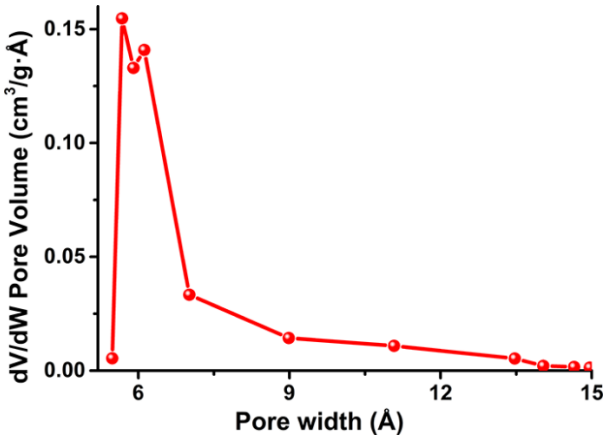

Fig. S8. The pore size distribution in structure **1**.

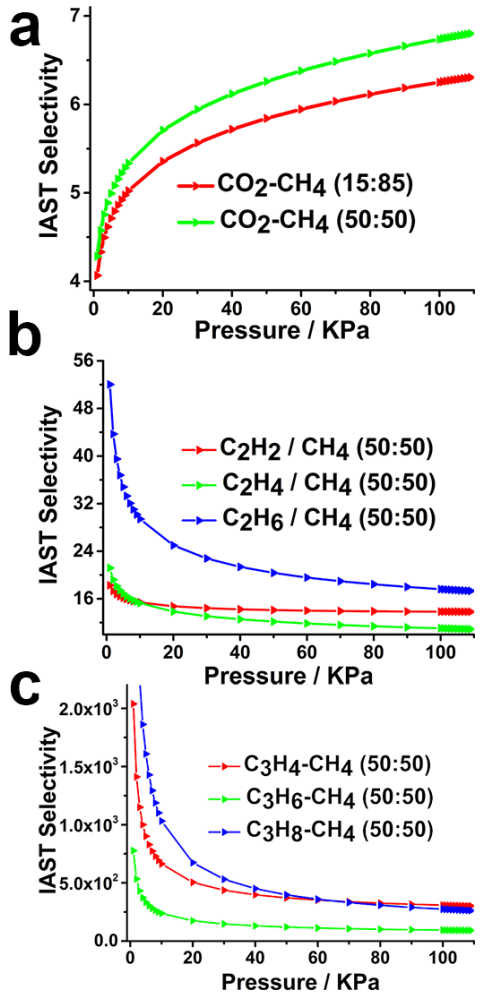

Fig. S9. (a) - (c) IAST predicted (50:50) gas mixture adsorption selectivities for **1** at 298 K and 1bar.

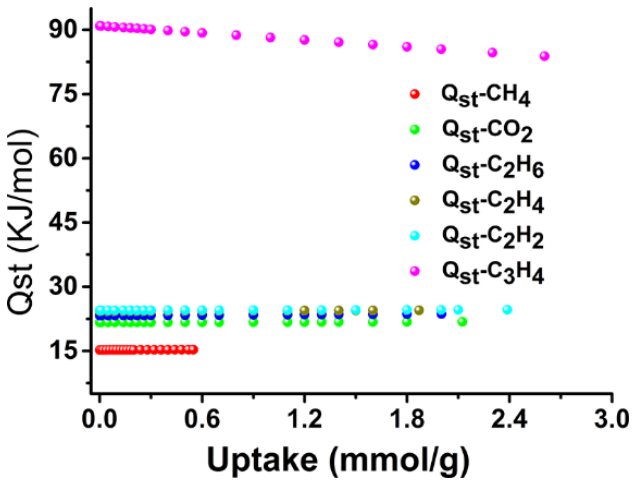

Fig. S10. The Q_{st} values for CH_4, CO_2, C_2H_6, C_2H_4, C_2H_2 and C_3H_4.

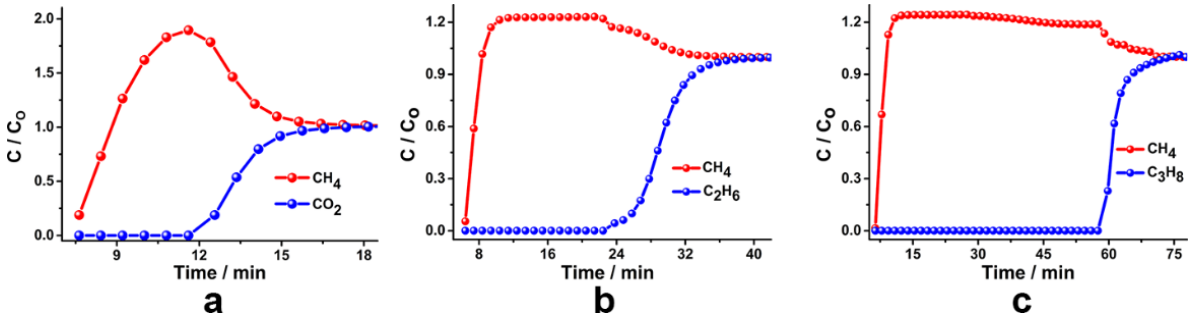

Fig. S11. Breakthrough curves for binary mixtures of CO_2/CH_4 (a), C_2H_6/CH_4 (b) and C_3H_8/CH_4 (c) (15:85) obtained for **1** at 298 K.

Tables

Table S1. Important crystal data of compound **1** (CCDC number: 1983688).

Identification code	**1**
Empirical formula	C8.75H9Ca0.50O2.62N0.25
Formula weight	179.7
Temperature	110 (2) K
Wavelength	1.54184 Å
Crystal system	tetragonal
Space group	*I*4/*m*
Unit cell dimensions	a = b = 13.8229(11) Å c = 24.906(2)
Volume	4758.9(9) $Å^3$
Z	16
Density (calculated)	1.003 g/cm^3
Absorption coefficient	2.449 mm^{-1}
F(000)	1508
Theta range for data collection	4.524 to 72.396°
Completeness to theta = 67.684°	98.7 %
Goodness-of-fit on F^2	1.034
Final R indices [I>2sigma(I)]	R1 = 0.0793, wR2 = 0.2485
R indices (all data)	R1 = 0.0826, wR2 = 0.2546
Largest diff. peak and hole	1.115 and -0.673 $e.Å^{-3}$

Table S2. Bond lengths [pm] and angles [°] of compound **1**.			
Ca(1)-O(1)#1	230.3(2)	Ca(1)-O(1)#3	259.1(2)
Ca(1)-O(1)#2	230.3(2)	Ca(1)-O(4)	259.68(15)
Ca(1)-O(3)	233.5(5)	Ca(2)-O(3)	153.6(6)
Ca(1)-O(2)	242.9(2)	Ca(2)-O(2)	233.3(3)
Ca(1)-O(3)	233.5(5)	Ca(2)-O(2)#3	233.3(3)
Ca(1)-O(2)	242.9(2)	Ca(2)-O(1)#1	254.1(3)
Ca(1)-O(2)#3	242.9(2)	Ca(2)-O(1)#2	254.1(3)
Ca(1)-O(1)	259.1(2)		

O(1)#1-Ca(1)-O(1)#2	81.05(12)	O(2)-Ca(1)-O(4)	116.08(7)
O(1)#1-Ca(1)-O(3)	86.37(12)	O(2)#3-Ca(1)-O(4)	116.08(7)
O(1)#2-Ca(1)-O(3)	86.37(12)	O(1)-Ca(1)-O(4)	67.09(6)
O(1)#1-Ca(1)-O(2)	166.19(9)	O(1)#3-Ca(1)-O(4)	67.09(6)
O(1)#2-Ca(1)-O(2)	90.24(8)	O(3)-Ca(2)-O(2)	106.54(19)
O(3)-Ca(1)-O(2)	82.37(12)	Ca(1)-Ca(2)-O(2)#3	86.5(2)
O(1)#1-Ca(1)-O(2)#3	90.24(8)	O(3)-Ca(2)-O(2)#3	106.54(19)
O(1)#2-Ca(1)-O(2)#3	166.19(9)	O(2)-Ca(2)-O(2)#3	101.53(19)
O(3)-Ca(1)-O(2)#3	82.37(12)	Ca(1)-Ca(2)-O(1)#1	64.16(16)
O(2)-Ca(1)-O(2)#3	96.14(13)	O(3)-Ca(2)-O(1)#1	99.3(2)
O(1)#1-Ca(1)-O(1)	138.19(11)	O(2)-Ca(2)-O(1)#1	149.1(2)
O(1)#2-Ca(1)-O(1)	89.70(11)	O(2)#3-Ca(2)-O(1)#1	86.87(9)
O(3)-Ca(1)-O(1)	133.92(10)	Ca(1)-Ca(2)-O(1)#2	64.16(16)
O(2)-Ca(1)-O(1)	51.72(7)	O(3)-Ca(2)-O(1)#2	99.3(2)
O(2)#3-Ca(1)-O(1)	103.88(8)	O(2)-Ca(2)-O(1)#2	86.87(9)
O(1)#1-Ca(1)-O(1)#3	89.70(11)	O(2)#3-Ca(2)-O(1)#2	149.1(2)
O(1)#2-Ca(1)-O(1)#3	138.19(11)	O(1)#1-Ca(2)-O(1)#2	72.16(13)
O(3)-Ca(1)-O(1)#3	133.92(10)	Ca(1)#4-O(4)-Ca(1)#2	180.00(6)
O(2)-Ca(1)-O(1)#3	103.88(8)	Ca(1)#4-O(4)-Ca(1)#5	90.0
O(2)#3-Ca(1)-O(1)#3	51.72(7)	Ca(1)#2-O(4)-Ca(1)#5	90.0
O(1)-Ca(1)-O(1)#3	70.55(10)	Ca(1)#4-O(4)-Ca(1)	90.0
O(1)#1-Ca(1)-O(4)	71.33(6)	Ca(1)#2-O(4)-Ca(1)	90.0
O(1)#2-Ca(1)-O(4)	71.33(6)	Ca(1)#5-O(4)-Ca(1)	180.0
O(3)-Ca(1)-O(4)	150.31(15)		

Symmetry transformations used to generate equivalent atoms:

#1 -y+1,x-1,-z; #2 -y+1,x-1,z; #3 x,y,-z; #4 y+1,-x+1,-z; #5 -x+2,-y,-z; #6 -y+3/2,x-1/2,-z+1/2; #7 -x+2,-y+1,z; #8 y+1/2,-x+3/2,-z+1/2.

Table S3. Comparison of adsorption performance of MOFs adsorbents for C_3H_8, C_3H_6, C_3H_4, C_2H_6, C_2H_4, C_2H_2, CH_4, CO_2. (cm^3/g)

Compound	C_3H_8	C_3H_6	C_3H_4	C_2H_6	C_2H_4	C_2H_2	CH4	CO_2
[1]FJI-C1	141.9	-	-	87.4	64	93.8	9.7	41.2
[2]FJI-C4	71.5	-	-	66.3	70.1	61.4	18.4	60.3
[3]NUM3a	-	-	-	24	34	-	25	83
[4]LIFM-26	117	-	-	103	100	-	-	75
[5]BSF-1	43.5	-	-	35.2	36.6	52.6	10.5	39.7
[6]JLU-Liu5	70	-	-	71	-	-	16	52
[6]JLU-Liu6	57	-	-	49	-	-	13	43
[7]JLU-Liu18	116	-	-	92	-	-	12	-
[8]JLU-Liu22	93	-	-	74	-	-	16	95
[9]JUC-100	136	-	-	92.1	66.3	-	10.2	-
[9]JUC-103	122	-	-	85.6	66.9	-	11.7	-
[9]JUC-106	114	-	-	78.2	50	-	8.14	-
[10]JXNU-3(Tb)	-	-	-	-	-	-	9.6	40.9
[11]UPC-32	84.9	98.2	-	66.1	57.2	60.6	18.9	65.7
[12]UPC-100-In	118.9	135	-	119.3	107.2	120.2	11.7	-
[12]UPC-101-Al	137.5	154.5	-	111.7	103.2	132.1	24.4	-
[12]UPC-102-Zr	137.8	141.9	-	74	56.4	70.6	9.4	-
[13]MFM-202a	151.4	160.8	-	94.3	65	77.1	10.1	-
[14]FIR-7a-ht	162.2	-	-	90.9	59.1		10.3	-
[15]PCN-88	-	-	-	-	-	-	18	94
[16]PCN-224	184.8	-	-	65.6	-	-	10.8	-
[17]UPC-21	103	110.1	-	104.3	98.4	139.5	-	-
[18]UPC-33	93.6	94.3	-	34.9	31.1	44.4	6.9	31.8
[19]UPC-104.	232.8	253.9	-	133.8	108.7	131	18.1	-
[20]UTSA-33a	-	-	-	61.97	60.96	83.6	-	-
[21]USTA-35a	66.6	73.8	-	54.5	48.5	65.1	9.7	-
[22]UTSA-61a	-	-	-	-	-	-	6.8	27.7
[23]Yb-BPT	-	-	-	-	-	23.9	5.4	16.7
[24]UiO-67 (288K)	212.8	-	-	95.4	-	-	-	-
[25]ZIF-100	-	-	-	-	-	-	-	21.4
[26]SIFSIX-2-Cu	-	-	-	-	-	-	8.68	41
[27]M'MOF-20a	-	-	-	-	-	21	2.9	10
[28]Y-H_3TDPAT	-	-	-	-	-	100	17.5	70.1
[29]ZJU-31a	-	-	-	67.4	65.3	71.1	16.6	-
[30]ZJU-30a	-	-	-	47.7	44.3	52.6	13.9	-
[31]ZJNU-61a(Ho)	-	-	-	55.3	40.8	48	6.2	-
[32]ZJNU-100	-	-	-	-	-	149.1	20.8	83.1
This work	36.7	47.9	58.1	44.9	41.9	53.5	11.9	47.6

Table S4. Comparison of adsorption performance of MOFs adsorbents for pore volume and BET.

Compound	**pore volume**	**BET**
[1]FJI-C1	-	1726.3
[2]FJI-C4	0.27	690
[3]NUM3a	0.82	2111.2
[4]LIFM-26	0.59	1513
[5]BSF-1	0.25	535
[6]JLU-Liu5	0.35	707
[6]JLU-Liu6	0.26	544
[7]JLU-Liu18	0.65	1300
[8]JLU-Liu22	0.77	1487
[9]JUC-100	-	2040
[9]JUC-103	-	1484
[9]JUC-106	-	1122
[10]JXNU-3(Tb)	-	646
[11]UPC-32	0.41	1345
[12]UPC-100-In	0.64	1677.7
[12]UPC-101-Al	0.65	2083.8
[12]UPC-102-Zr	1.58	2182.5
[13]MFM-202a	-	2220
[14]FIR-7a-ht	0.684	1894.1
[15]PCN-88	-	3308
[16]PCN-224	1.06	2704
[17]UPC-21	-	1725.1
[18]UPC-33	0.5	933.8
[20]UTSA-33a	0.367	660
[21]USTA-35a	0.313	742.7
[33]UTSA-36a	0.33	495
[22]UTSA-61a	0.67	770
[23]Yb-BPT	0.291	515.6
[25]ZIF-100	0.37	595
[34]MIL-53(Al)	0.6	1463
[27]M'MOF-20a	0.022	42
[28]Y-H3TDPAT	0.42	962
[29]ZJU-31a	0.4	1115
[30]ZJU-30a	-	228
[31]ZJNU-61a(Ho)	0.456	1059
[32]ZJNU-100	0.754	1933
This work	0.24	531.8

Table S5. Comparison of gas separation of MOFs adsorbents for C_3H_8, C_3H_6, C_3H_4, C_2H_6, C_2H_4, C_2H_2 and CO_2 over CH_4

Compound	C_3H_8/CH_4	C_3H_6/CH_4	C_3H_4/CH_4	C_2H_6/CH_4	C_2H_4/CH_4	C_2H_2/CH_4	CO_2/CH_4
[1]FJI-C1 (50:50)	14.6	-	-	9	6.6	9.7	5.89
[2]FJI-C4 (50:50)	293	-	-	39.7	22.1	51	
[3]NUM3a (50:50)	-	-	-	-	-	-	11
[4]LIFM-26	46	-	-	11	23	-	36
[5]BSF-1 (50:50)	353	-	-	23	-	46.9	7.5
[6]JLU-Liu5 (50:50)	107.8	-	-	17.6	-	-	4.6
[6]JLU-Liu6 (50:50)	274.6	-	-	20.4	-	-	7.3
[7]JLU-Liu18	108.2	-	-	13.1	-	-	5.4/4.5
[8]JLU-Liu22 (50:50)	271.5	-	-	14.4	-	-	9.4
[9]JUC-100 (50:50)	65–150	-	-	8–16	-	-	-
[9]JUC-103 (50:50)		-	-		-	-	-
[9]JUC-106 (50:50)		-	-		-	-	-
[10]JXNU-3(Tb) (50:50)	-	-	-	-	-	-	21.5
[11]UPC-32	28	31.4	-	5.2	4.3	5.8	6.6
[12]UPC-100-In	186.4	200.5	-	-	-	-	-
[12]UPC-101-Al	37.2	32.5	-	-	-	-	-
[12]UPC-102-Zr	42.5	44	-	-	-	-	-
[13]MFM-202a	87	75	-	12-7			-
[14]FIR-7a-ht	78.8	-	-	14.6	8.6	-	-
[15]PCN-88	-	-	-	-	-	-	7
[16]PCN-224	609	-	-	12	-	-	-
[17]UPC-21 (50:50)	67	75	-	15.3	23.5	38.1	-
[18]UPC-33 (50:50)	41.77	42.4	-	4.8	4.48	7.78	8.09
[19]UPC-104	79	97.9	-	12.3	8.9	11.8	-
[20]UTSA-33a	-	-	-	4.8	4.7	6.5	-

[21]USTA-35a (5:95)	excess 80	-	-	excess 8			-
[33]UTSA-36a	-	-	-	16.6	11.1	13.8	-
[22]UTSA-61a	-	-	-	-	-	-	7.4
[23]Yb-BPT	-	-	-	-	-	7.8	3.1
[24]UiO-67 (288K)	73.7	-	-	8.1	-	-	-
[25]ZIF-100 (50:50)	-	-	-	-	-	-	5.9
[26]SIFSIX-2-Cu	-	-	-	-	-	-	5.3
[34]MIL-53(Al)	-	-	-	-	-	-	-
[27]M'MOF-20a (50:50)	-	-	-	-	-	34.9	6.8
[34]ZIF-8	-	-	-	-	-	-	1.32
[35]MOF-177 (50:50)	-	-	-	-	-	-	4.4
[34]$Cu_3(BTC)_2$	-	-	-	-	-	-	2.28
[28]Y-H3TDPAT	-	-	-	-	-	77.2	9.7
[29]ZJU-31a	-	-	-	23.4	22	22.5	-
[30]ZJU-30a	-	-	-	19.5	11.5	9.58	-
[31]ZJNU-61a(Ho)	-	-	-	11.1	7.8	9.9	-
ZJNU-100	-	-	-	-	-	22.2	5.13
This work (15:85)	502.3	140.1	422.4	21.4	12.4	14.2	6.305
This work (50:50)	261.4	91.3	302	17.3	13.8	10.9	6.8

References

1 Y. Huang, Z. Lin, H. Fu, F. Wang, M. Shen, X. Wang and R. Cao, *ChemSusChem*, 2014, **7**, 2647-2653.

2 L. Li, X. Wang, J. Liang, Y. Huang, H. Li, Z. Lin and R. Cao, *ACS Appl. Mater. Interfaces*, 2016, **8**, 9777-9781.

3 M. H. Yu, P. Zhang, R. Feng, Z. Q. Yao, Y. C. Yu, T. L. Hu and X. H. Bu, *ACS Appl. Mater. Interfaces*, 2017, **9**, 26177-26183.

4 C. X. Chen, S. P. Zheng, Z. W. Wei, C. C. Cao, H. P. Wang, D. Wang, J. J. Jiang, D. Fenske and C. Y. Su, *Chem. Eur. J.* , 2017, **23**, 4060-4064.

5 Y. Zhang, L. Yang, L. Wang, S. Duttwyler and H. Xing, *Angew. Chem. Int. Ed.* ,

2019, **58**, 8145-8150.
6 D. Wang, T. Zhao, Y. Cao, S. Yao, G. Li, Q. Huo and Y. Liu, *Chem. Commun.*, 2014, **50**, 8648-8650.
7 S. Yao, D. Wang, Y. Cao, G. Li, Q. Huo and Y. Liu, *J. Mater. Chem. A*, 2015, **3**, 16627-16632.
8 D. Wang, B. Liu, S. Yao, T. Wang, G. Li, Q. Huo and Y. Liu, *Chem. Commun.*, 2015, **51**, 15287-15289.
9 J. Jia, L. Wang, F. Sun, X. Jing, Z. Bian, L. Gao, R. Krishna and G. Zhu, *Chem. Eur. J.*, 2014, **20**, 9073-9080.
10 Y. J. Li, Y. L. Wang and Q. Y. Liu, *Inorg Chem*, 2017, **56**, 2159-2164.
11 W. Fan, Y. Wang, Z. Xiao, Z. Huang, F. Dai, R. Wang and D. Sun, *Chinese Chem. Lett*, 2018, **29**, 865-868.
12 W. Fan, X. Wang, B. Xu, Y. Wang, D. Liu, M. Zhang, Y. Shang, F. Dai, L. Zhang and D. Sun, *J. Mater. Chem. A*, 2018, **6**, 24486-24495.
13 S. Gao, C. G. Morris, Z. Lu, Y. Yan, H. G. W. Godfrey, C. Murray, C. C. Tang, K. M. Thomas, S. Yang and M. Schröder, *Chem. Mater.*, 2016, **28**, 2331-2340.
14 Y. P. He, Y. X. Tan and J. Zhang, *Chem. Commun.*, 2013, **49**, 11323-11325.
15 J. R. Li, J. Yu, W. Lu, L. B. Sun, J. Sculley, P. B. Balbuena and H. C. Zhou, *Nat. Commun.*, 2013, **4**, 1538.
16 R. Shi, D. Lv, Y. Chen, H. Wu, B. Liu, Q. Xia and Z. Li, *Sep. Purif. Technol.*, 2018, **207**, 262-268.
17 M. Zhang, X. Xin, Z. Xiao, R. Wang, L. Zhang and D. Sun, *Journal of Materials Chemistry A*, 2017, **5**, 1168-1175.
18 W. Fan, Y. Wang, Q. Zhang, A. Kirchon, Z. Xiao, L. Zhang, F. Dai, R. Wang and D. Sun, *Chem. Eur. J.*, 2018, **24**, 2137-2143.
19 W. Fan, X. Liu, X. Wang, Y. Li, C. Xing, Y. Wang, W. Guo, L. Zhang and D. Sun, *Inorg. Chem. Front.*, 2018, **5**, 2445-2449.
20 Y. He, Z. Zhang, S. Xiang, F. R. Fronczek, R. Krishna and B. Chen, *Chem. Eur. J.*, 2012, **18**, 613-619.
21 Y. He, Z. Zhang, S. Xiang, F. R. Fronczek, R. Krishna and B. Chen, *Chem. Commun.*, 2012, **48**, 6493-6495.
22 Y. He, H. Furukawa, C. Wu, M. O'Keeffe and B. Chen, *CrystEngComm*, 2013, **15**, 9328–9331.
23 Z. Guo, H. Xu, S. Su, J. Cai, S. Dang, S. Xiang, G. Qian, H. Zhang, M. O'Keeffe and B. Chen, *Chem. Commun.* , 2011, **47**, 5551-5553.
24 Y. Zhang, H. Xiao, X. Zhou, X. Wang and Z. Li, *Ind. Eng. Chem. Res.*, 2017, **56**, 8689-8696.
25 B. Wang, A. P. Cote, H. Furukawa, M. O'Keeffe and O. M. Yaghi, *Nature*, 2008, **453**, 207-211.
26 P. Nugent, Y. Belmabkhout, S. D. Burd, A. J. Cairns, R. Luebke, K. Forrest, T. Pham, S. Ma, B. Space, L. Wojtas, M. Eddaoudi and M. J. Zaworotko, *Nature*, 2013, **495**, 80-84.
27 Z. Zhang, S. Xiang, K. Hong, M. C. Das, H. D. Arman, M. Garcia, J. U. Mondal, K. M. Thomas and B. Chen, *Inorg Chem*, 2012, **51**, 4947-4953.

28 K. Liu, X. Li, D. Ma, Y. Han, B. Li, Z. Shi, Z. Li and L. Wang, *Mater. Chem. Front*., 2017, **1**, 1982-1988.
29 J. Cai, J. Yu, H. Wang, X. Duan, Q. Zhang, C. Wu, Y. Cui, Y. Yu, Z. Wang, B. Chen and G. Qian, *Cryst. Growth Des.*, 2015, **15**, 4071-4074.
30 J. Cai, J. Yu, H. Xu, Y. He, X. Duan, Y. Cui, C. Wu, B. Chen and G. Qian, *Crystal Growth & Design*, 2013, **13**, 2094-2097.
31 Y. Ling, J. Jiao, M. Zhang, H. Liu, D. Bai, Y. Feng and Y. He, *Cryst. Eng. Comm*, 2016, **18**, 6254-6261.
32 Y. Wang, M. He, X. Gao, X. Wang, G. Xu, Z. Zhang and Y. He, *Inorganic Chemistry Frontiers*, 2019, **6**, 263-270.
33 M. C. Das, H. Xu, S. Xiang, Z. Zhang, H. D. Arman, G. Qian and B. Chen, *Chem. Eur. J.*, 2011, **17**, 7817-7822.
34 Z. Xiang, X. Peng, X. Cheng, X. Li and D. Cao, *The Journal of Physical Chemistry C*, 2011, **115**, 19864-19871.
35 D. Saha , Z. Bao , F. Jia , and S. G. Deng, *Environ. Sci. Technol.*, 2010, **44**, 1820–1826.